

Article

Design, Synthesis, and Spectral Properties of Novel 2-Mercaptobenzothiazole Derivatives

Agnieszka Skotnicka *  and Janina Kabatc-Borcz 

Faculty of Chemical Technology and Engineering, Bydgoszcz University of Science and Technology, Seminaryjna 3, 85-326 Bydgoszcz, Poland; nina@pbs.edu.pl

* Correspondence: askot@pbs.edu.pl; Tel.: +48-523749111

Abstract: This paper is focused on the optimization of methods for the synthesis, isolation, and purification of 2-mercaptobenzothiazole-based acrylic and methacrylic monomers. The structures of the newly synthesized compounds were confirmed through infrared (IR) and nuclear magnetic resonance spectroscopy (NMR). Spectroscopic properties of the resulting 2-mercaptobenzothiazole derivatives were determined based on their absorption spectra and molar absorption coefficients in solvents with varying polarities. A correlation was established between the calculated density functional theory (DFT) energies and Frontier Molecular Orbitals and the experimental observations, confirming their consistency. The practical utility of the synthesized compounds, particularly in future polymerization processes, hinges on a thorough understanding of these properties.

Keywords: 2-mercaptobenzothiazole; synthesis; spectroscopic properties; quantum chemical calculations

1. Introduction

The 2-mercaptobenzothiazoles (MBT) (Figure 1) constitute a significant group of bioactive and industrially crucial organic compounds. It is noteworthy that their derivatives are of huge interest in scientific research owing to their potential pharmacological properties [1]. The widespread use of these substances in the medical field, such as their application as anti-inflammatory [2], antibacterial [3,4], and antifungal agents [5], along with their efficacy in treating diseases such as cancer and cardiovascular illnesses [6], has garnered considerable attention. The interest in this group of compounds arises not only from their medicinal applications but also from their diverse uses in various industries: 2-mercaptobenzothiazole serves as a widely utilized organic corrosion inhibitor [7] for copper [8,9] and zinc [10,11], and as a component of self-healing and anticorrosion smart coatings [12–15]. Larsson et al. [16] suggested that MBT can serve as an additive in dye solar devices. Moreover, 2-mercaptobenzothiazole and its derivative zinc 2-mercaptobenzothiazole (ZMBT) [17] are commonly used as ‘hemi-ultra’ accelerators in the vulcanization process of both natural and synthetic rubber. Additionally, they find applications as plasticizers in the rubber industry [18–20]. Heteroaromatic thiols, including MBT, among others, have been utilized as co-initiators for type II photo-initiators composed of camphoroquinone and isopropylthioxanthone. Kinetic data indicate their efficiency as co-initiators, comparable to aromatic amines. Due to their ability to readily donate hydrogen atoms, some of these thiols have been employed as co-initiators of hexaarylbisimidazoles (HABI) [21]. In other study, Degirmenci et al. copolymerized a methacrylic monomer containing a benzothiazole disulfide group with a hydrophilic polyethylene glycol (PEG)-based monomer, resulting in a redox-responsive functional polymer. The straightforward synthesis of these copolymers, which are highly functionalizable, and their application in the preparation of reversibly functionalizable coatings, establishes a versatile interface for a range of biomedical applications [22].



Citation: Skotnicka, A.; Kabatc-Borcz, J. Design, Synthesis, and Spectral Properties of Novel 2-Mercaptobenzothiazole Derivatives. *Materials* **2024**, *17*, 246. <https://doi.org/10.3390/ma17010246>

Academic Editor: Georgios Bokias

Received: 29 November 2023

Revised: 25 December 2023

Accepted: 26 December 2023

Published: 2 January 2024



Copyright: © 2024 by the authors. Licensee MDPI, Basel, Switzerland. This article is an open access article distributed under the terms and conditions of the Creative Commons Attribution (CC BY) license (<https://creativecommons.org/licenses/by/4.0/>).

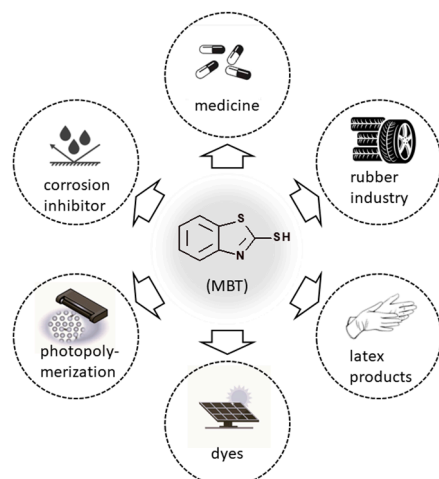


Figure 1. Examples of applications of 2-mercaptobenzothiazole.

Acrylic acid derivatives, commonly referred to as acrylates, encompass salts and esters derived from acrylic and methacrylic acid. Characterized by a vinyl group linked to a carboxyl group, these compounds undergo facile polymerization owing to an active double bond within their structure. As monomers, they rank among the most widely employed in the synthesis of polymeric plastics. The inherent compatibility of acrylic and methacrylic monomers facilitates polymerization not only with each other but also with diverse monomers, thereby contributing to the fabrication of numerous polymer compositions [23,24]. Manipulating the composition and proportions allows for the production of materials with varied final properties [25]. Acrylic polymers, renowned for their diverse properties, encompassing excellent durability, transparency, strength, UV stability, ease of dyeing, and color fastness, find extensive utility in the production of various commodities. These polymers play pivotal roles in optics [26] and medicine [27,28] and numerous industries, notably in the manufacturing of paints and adhesives [29], for the design of macromolecular self-organizing materials [30,31], as well as applications in the textile industry. Their versatility extends across a spectrum of forms, ranging from very soft adhesive materials to loose powders, and even to rigid, hard boards and consumer products.

The distinctive characteristics of 2-mercaptobenzothiazole and its acrylic and methacrylic acid derivatives motivated the development of a novel group of compounds (Figure 2). These newly synthesized compounds can be regarded as functional monomers, showing potential applications in the expansive domains of polymer chemistry and technology. The objectives of this paper is the synthesis and study on the structures and spectroscopic properties of the new compounds based on 2-mercaptobenzothiazole. It is assumed that the indicated acrylate and methacrylate derivatives of 2-mercaptobenzothiazole have the potential to serve as photo-initiators of radical polymerization of various acrylate monomers. Furthermore, some of these compounds can be used as photo-initiators, as well as serve as attractive building units and components for advanced polymeric materials with a high refractive index. Examples of such applications include their use in foldable intraocular lenses [32] and for industrial applications, such as coatings [33,34].

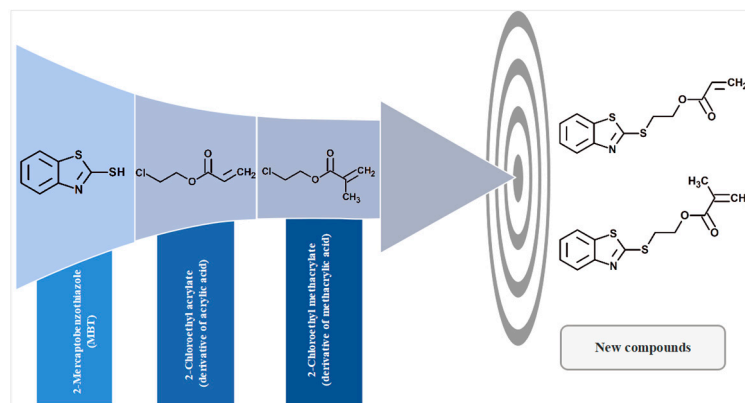


Figure 2. New compounds based on 2-mercaptobenzothiazole and derivatives of (meth)acrylic acid.

2. Materials and Methods

2.1. Materials

All the reagents and solvents were purchased from Sigma-Aldrich (Poznań, Poland) and utilized without additional purification. The spectroscopic studies necessitated the use of chemicals with the highest purity ($\geq 99\%$).

2.2. Synthesis

The synthesis followed the methodology outlined in [33]. The method of purification was modified. Substituted 2-mercaptobenzothiazole (28 mmol) and sodium bicarbonate (28.5 mmol, 2.4 g) were dissolved in 10 mL of dimethylformamide at 60 °C. Then, 2-chloroethyl acrylate (29 mmol, 3.47 mL) or 2-chloroethyl methacrylate (29 mmol, 2.93 mL) was added, dropwise. The reaction mixture was refluxed overnight, washed with a 5% NaOH aqueous solution, and extracted with diethyl ether. The organic layer was separated and dried using MgSO_4 , filtered, and the solvent was removed under vacuum. The crude oil underwent purification through silica gel column chromatography using dichloromethane as the eluent, with fractions collected at 285 nm.

Elemental Analysis

Elemental analysis was as follows:

2-(2-(6-Methylbenzothiazolyl)thio)ethyl acrylate (**1**). Bp 238.7 °C, yellow oil. IR (ATR), cm^{-1} : 3031–3425, 2860–2951, 1720, and 1632. λ_{abs} : 283 nm (DCM). ^1H NMR (400 MHz, CDCl_3) δ (ppm): 7.72 (d, 1H, $^3J_{\text{H,H}} = 8.28$ Hz, Ar), 7.51 (s, 1H, Ar), 7.21 (m, 1H, Ar), 6.41 (d, 1H, $^3J_{\text{H,H}} = 17.32$ Hz, $\text{CH}=\text{CH}_2$), 6.11 (q, 1H, $\text{CH}=\text{CH}_2$), 5.82 (d, 1H, $^3J_{\text{H,H}} = 10.48$ Hz, $\text{CH}=\text{CH}_2$), 4.53 (t, 2H, $\text{CH}_2\text{-O}$), 3.63 (t, 2H, S-CH_2), 2.39 (t, 3H, CH_3). ^{13}C NMR (100 MHz, CDCl_3) δ (ppm): 165.8, 164.1, 151.1, 135.5, 134.6, 131.2, 128.0, 127.6, 121.1, 120.9, 62.3, 31.9, 21.4. $\text{C}_{13}\text{H}_{13}\text{NO}_2\text{S}_2$, Calcd. C, 55.89, H, 4.69, N, 5.01, S, 22.95. Found C, 55.45, H, 6.70, N, 4.83, S, 23.36, M^+ : 279.1 (Supplementary Materials).

2-(2-(6-Chlorobenzothiazolyl)thio)ethyl acrylate (**2**). Bp 251.9 °C, light orange oil. IR (ATR), cm^{-1} : 3036–3435, 2690–2946, 1720, and 1633. λ_{abs} : 285 nm (DCM). ^1H NMR (400 MHz, CDCl_3) δ (ppm): 7.67 (d, 1H, $^3J_{\text{H,H}} = 8.68$ Hz, Ar), 7.63 (d, 1H, $^3J_{\text{H,H}} = 1.92$ Hz, Ar), 7.29 (dd, 1H, Ar), 6.34 (d, 1H, $^3J_{\text{H,H}} = 17.32$ Hz, $\text{CH}=\text{CH}_2$), 6.04 (q, 1H, $\text{CH}=\text{CH}_2$), 5.76 (d, 1H, $^3J_{\text{H,H}} = 10.44$ Hz, $\text{CH}=\text{CH}_2$), 4.46 (t, 2H, $\text{CH}_2\text{-O}$), 3.58 (t, 2H, S-CH_2). ^{13}C NMR (100 MHz, CDCl_3) δ (ppm): 166.2, 165.7, 151.6, 136.5, 131.3, 130.2, 128.0, 127.8, 122.2, 120.6, 62.6, 31.9. $\text{C}_{12}\text{H}_{10}\text{ClNO}_2\text{S}_2$, Calcd. C, 48.08, H, 3.36, N, 4.67, S, 21.39. Found C, 48.2, H, 3.56, N, 4.59, S, 21.15, M^+ : 299.0 (Supplementary Materials).

2-(2-(5-Chlorobenzothiazolyl)thio)ethyl acrylate (**3**). Bp 252.4 °C, yellow oil. IR (ATR), cm^{-1} : 3035–3435, 2658–2947, 1721, and 1634. λ_{abs} : 279 nm (DCM). ^1H NMR (400 MHz, CDCl_3) δ (ppm): 7.76 (s, 1H, Ar), 7.56 (d, 1H, $^3J_{\text{H,H}} = 8.48$ Hz, Ar), 7.19 (d, 1H, $^3J_{\text{H,H}} = 7.8$ Hz, Ar), 6.35 (d, 1H, $^3J_{\text{H,H}} = 17.32$ Hz, $\text{CH}=\text{CH}_2$), 6.04 (q, 1H, $\text{CH}=\text{CH}_2$), 5.77

(d, 1H, $^3J_{H,H} = 10.44$ Hz, CH=CH₂), 4.47 (t, 2H, CH₂-O), 3.60 (t, 2H, S-CH₂). ¹³C NMR (100 MHz, CDCl₃) δ (ppm): 167.7, 165.6, 153.7, 133.5, 132.0, 131.2, 127.9, 124.6, 121.5, 121.3, 62.4, 31.7. C₁₂H₁₀ClNO₂S₂, Calcd. C, 48.08, H, 3.36, N, 4.67, S, 21.39. Found C, 48.25, H, 3.53, N, 4.0, S, 21.66, M⁺: 299.0 (Supplementary Materials).

2-(2-(6-Methylbenzothiazolyl)thio)ethyl methacrylate (4). Bp 248.1 °C, dark brown oil. IR (ATR), cm⁻¹: 2950–3021, 2734–2922, 1715, and 1636. λ_{abs}: 285 nm (DCM). ¹H NMR (400 MHz, CDCl₃) δ (ppm): 7.65 (d, 1H, $^3J_{H,H} = 8.08$ Hz, Ar), 7.44 (s, 1H, Ar), 7.12 (dd, 1H, Ar), 6.03 (s, 1H, C(CH₃)=CH₂), 5.47 (s, 1H, C(CH₃)=CH₂), 4.44 (t, 2H, CH₂-O), 3.56 (t, 2H, S-CH₂), 2.36 (s, 3H, CH₃), 1.83 (s, 3H, C(CH₃)=CH₂). ¹³C NMR (100 MHz, CDCl₃) δ (ppm): 167.0, 164.2, 151.2, 136.0, 135.5, 134.5, 127.5, 126.0, 121.1, 120.8, 62.9, 31.9, 21.4, 18.2. C₁₄H₁₅NO₂S₂, Calcd. C, 57.31, H, 5.15, N, 4.77, S, 21.86. Found C, 57.01, H, 5.30, N, 5.07, S, 21.71, M⁺: 293.1 (Supplementary Materials).

2-(2-(6-Chlorobenzothiazolyl)thio)ethyl methacrylate (5). Bp 274.1 °C, brown oil. IR (ATR), cm⁻¹: 2951–3021, 2734–2922, 1715, and 1636. λ_{abs}: 285 nm (DCM). ¹H NMR (400 MHz, CDCl₃) δ (ppm): 7.78 (d, 1H, $^3J_{H,H} = 8.68$ Hz, Ar), 7.75 (d, 1H, $^3J_{H,H} = 2.08$ Hz, Ar), 7.40 (dd, 1H, Ar), 6.13 (s, 1H, C(CH₃)=CH₂), 5.58 (s, 1H, C(CH₃)=CH₂), 4.55 (t, 2H, CH₂-O), 3.69 (t, 2H, S-CH₂), 1.94 (s, 3H, C(CH₃)=CH₂). ¹³C NMR (100 MHz, CDCl₃) δ (ppm): 167.0, 166.4, 151.6, 136.5, 135.9, 130.3, 126.8, 126.0, 122.2, 120.6, 62.7, 32.0, 18.2. C₁₃H₁₂ClNO₂S₂, Calcd. C, 49.75, H, 3.85, N, 4.46, S, 20.44. Found C, 49.90, H, 4.00, N, 4.31, S, 20.29, M⁺: 313.0 (Supplementary Materials).

2-(2-(5-Chlorobenzothiazolyl)thio)ethyl methacrylate (6). Bp 280.7 °C, orange oil. IR (ATR), cm⁻¹: 3066–3085, 2836–2978, 1714, and 1636. λ_{abs}: 279 nm (DCM). ¹H NMR (400 MHz, CDCl₃) δ (ppm): 7.77 (s, 1H, Ar), 7.57 (d, 1H, $^3J_{H,H} = 8.48$ Hz, Ar), 7.20 (dd, 1H, Ar), 6.04 (s, 1H, C(CH₃)=CH₂), 5.49 (s, 1H, C(CH₃)=CH₂), 4.46 (t, 2H, CH₂-O), 3.60 (t, 2H, S-CH₂), 1.85 (s, 3H, C(CH₃)=CH₂). ¹³C NMR (100 MHz, CDCl₃) δ (ppm): 167.9, 167.0, 153.8, 135.9, 133.5, 132.2, 126.0, 124.7, 121.6, 121.4, 62.7, 31.9, 18.2. C₁₃H₁₂ClNO₂S₂, Calcd. C, 49.75, H, 3.85, N, 4.46, S, 20.44. Found C, 49.40, H, 4.14, N, 4.17, S, 20.79, M⁺: 313.0 (Supplementary Materials).

2.3. Experimental Measurements

2.3.1. NMR Measurements

The ¹H and ¹³C NMR spectra were measured on a Bruker Ascend III spectrometer operating at 400 MHz (Bydgoszcz, Poland). Chloroform served as the solvent, and tetramethylsilane (TMS) was used as the internal standard. Chemical shifts (δ) are reported in ppm relative to TMS and coupling constants (J) are expressed in Hz.

2.3.2. Elemental Analysis Measurements

Elemental analysis was performed using a Vario MACRO 11.45–0000 Elemental Analyzer System, GmbH (Toruń, Poland), with VARIOEL software (version 5.14.4.22).

2.3.3. UV-Vis Measurements

The absorption spectra were measured at room temperature in a quartz cuvette (1 cm) using an Agilent Technology UV-Vis Cary 60 Spectrophotometer (Bydgoszcz, Poland).

2.3.4. FT-IR Measurements

Infrared spectra were measured using an Alpha Bruker's compact FT-IR spectrometer equipped with diamond ATR, covering the range of 4000–360 cm⁻¹ (Bydgoszcz, Poland).

2.3.5. Boiling Point

The boiling point was measured on the Melting Point M-565 Apparatus (Buchi; Bydgoszcz, Poland) with the following parameters: temperature gradient 5.0 °C/min, barometric pressure 1013 mbar, and boiling frequency 0.6 Hz.

2.3.6. GC-MS Measurements

Chromatographic analyses were performed using an Agilent 7890B (Bydgoszcz, Poland), equipped with a split/splitless injector and multipurpose autosampler, and an Agilent 5977B mass-selective detector. The GC was fitted with a ZB-5-MS column (Zebtron, Phenomenex Inc., Torrance, CA, USA), 30 m × 0.25 mm 0.25 μm, containing (5% phenyl)-methylpolysiloxane.

The injector port was held at 270 °C and used in the split mode (5:1), and 1 μL injections were made. The temperature program used for the analysis was as follows: 80 °C (2 min), ramped at 15 °C/min to 250 °C, and held for 15 min. Helium was used as the carrier gas at a flow rate of 1 mL min⁻¹.

Full-scan mass spectra were recorded with an *m/z* range of 50–400 in electron-impact mode at 70 eV.

The transfer line and ion source temperatures were set at 280 and 230 °C, respectively. The scan rate was 2.9 scan/s, with a cathode delay time of 5 min. The SCAN mode was used for identification of analytes.

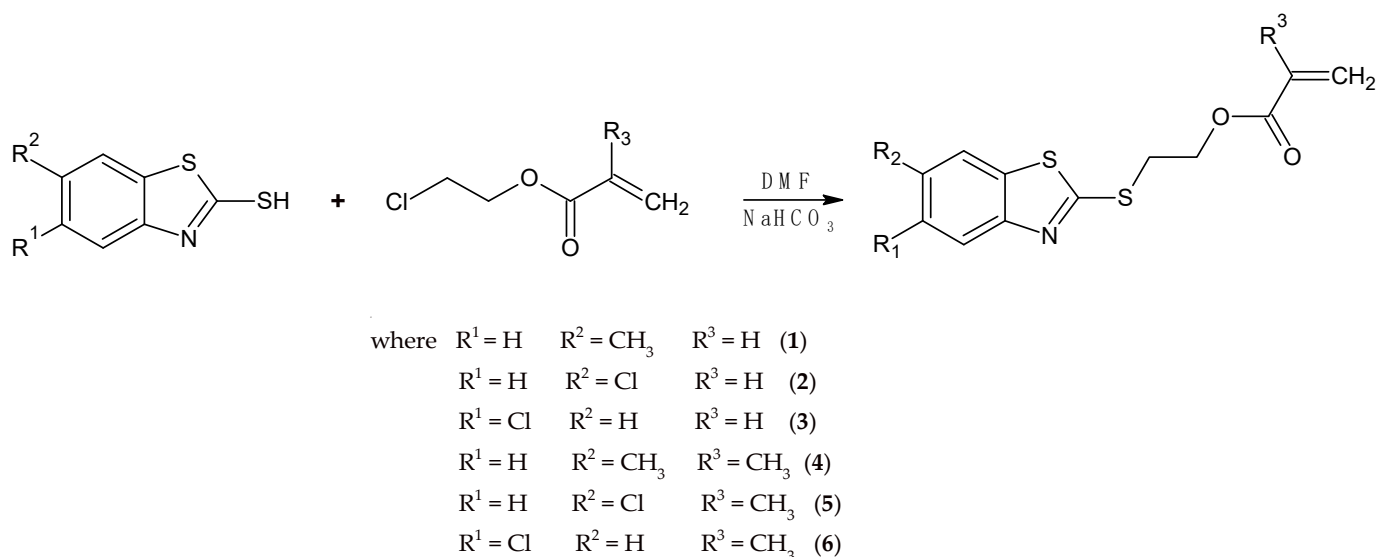
2.3.7. Quantum Mechanical Calculations

Geometry optimization, vibrational spectra, and the energies of the Highest Occupied Molecular Orbital (HOMO) and Lowest Unoccupied Molecular Orbital (LUMO) were calculated using density functional theory (DFT) with the B3LYP [35–37] functional and 6–311+G(d,p) basis set [38,39]. The calculations were performed using Gaussian 09 software [40]. Analysis of frontier orbitals and FT-IR spectra was conducted using the Avogadro 1.2.0 application [41].

3. Results and Discussion

3.1. Synthesis and NMR Data

The 2-(2-benzothiazolylthio)ethyl acrylate derivatives (1–3) and methacrylate derivatives (4–6) presented in this paper were synthesized following the method proposed by Macaskie et al. [33], as depicted in Scheme 1.



Scheme 1. Synthesis procedure for 2-(2-benzothiazolylthio)ethyl acrylate (1–3) and methacrylate derivatives (4–6).

The final products were separated and obtained in the form of oils, and were then purified via flash chromatography using dichloromethane as the eluent.

The structures and purity of the obtained compounds were confirmed through nuclear magnetic resonance spectra, including ¹H and ¹³C isotopes, as well as ¹H-¹³C HMQC and ¹H-¹³C HMBC spectra. The most characteristic chemical shifts for ¹H and ¹³C NMR are collected in

Tables 1 and 2, respectively. The $^1\text{H-NMR}$ signals for $=\text{CH}_2$ in acrylic 2-mercaptobenzothiazole derivatives (1–3) appeared as doublets at $\delta = 5.75\text{--}6.41$ ppm in CDCl_3 . The same protons in methacrylate derivatives (4–6) exhibited signals at $\delta = 5.47\text{--}6.13$ ppm in CDCl_3 , appearing as a singlet (Figure 3). An adjacent hydrogen atom bonded to a carbon involved in the formation of a carbon–carbon double bond appeared at approximately 6 ppm as a quartet. Alkyl protons from CH_2 groups were observed at around 4.5 ppm and 3.5 ppm for $\text{CH}_2\text{-O}$ and $\text{CH}_2\text{-S}$, respectively. They were present as triplets in both cases. Hydrogen atoms bonded to the aromatic ring were observed in the characteristic range for aromatic protons from 7 to 8 ppm. These chemical shift values and signal patterns align with those previously reported by us for related compounds [42].

Table 1. ^1H NMR chemical shifts for 2-(2-benzothiazolylthio)ethyl acrylate derivatives (1–3) and methacrylate (4–6) derivatives in 0.1–0.2 M solutions in CDCl_3 (measured), CDCl_3 , and $\text{DMSO-}d_6$ (italic, calculated) at 303 K.

Compound	Solvent	$\text{CH}=\text{CH}_2/\text{C}(\text{CH}_3)=\text{CH}_2$	$\text{CH}=\text{CH}_2$	$\text{C}(\text{CH}_3)=\text{CH}_2$	$\text{CH}_2\text{-O}$	S-CH_2
1	CHCl_3	6.41; 5.82	6.11	-	4.53	3.63
	<i>CHCl_3</i>	7.24; 6.48	6.58	-	4.42	3.47
	<i>$\text{DMSO-}d_6$</i>	7.23; 6.56	6.68	-	4.52	3.51
2	CHCl_3	6.34; 5.76	6.04	-	4.46	3.58
	<i>CHCl_3</i>	7.12; 6.29	6.47	-	4.38	3.46
	<i>$\text{DMSO-}d_6$</i>	7.02; 6.37	6.59	-	4.44	3.53
3	CHCl_3	6.35; 5.75	6.04	-	4.47	3.60
	<i>CHCl_3</i>	7.12; 6.41	6.44	-	4.40	3.48
	<i>$\text{DMSO-}d_6$</i>	7.01; 6.38	6.58	-	4.42	3.53
4	CHCl_3	6.03; 5.47	-	1.83	4.44	3.56
	<i>CHCl_3</i>	7.38; 6.17	-	2.27	4.84	3.46
	<i>$\text{DMSO-}d_6$</i>	7.36; 6.24	-	2.30	4.93	3.49
5	CHCl_3	6.13; 5.58	-	1.94	4.55	3.69
	<i>CHCl_3</i>	6.81; 6.12	-	2.22	4.34	3.61
	<i>$\text{DMSO-}d_6$</i>	6.77; 6.08	-	2.15	4.29	3.56
6	CHCl_3	6.04; 5.49	-	1.85	4.46	3.60
	<i>CHCl_3</i>	6.56; 5.84	-	2.24	4.47	3.63
	<i>$\text{DMSO-}d_6$</i>	6.70; 5.93	-	2.14	4.42	3.57

Table 2. ^{13}C NMR chemical shifts of 2-(2-benzothiazolylthio)ethyl acrylate derivatives (1–3) and methacrylate derivatives (4–6) for 0.1–0.2 M solutions in CDCl_3 (measured), CDCl_3 , and $\text{DMSO-}d_6$ (italic, calculated) at 303 K.

Compound	Solvent	$\text{CH}=\text{CH}_2/\text{C}(\text{CH}_3)=\text{CH}_2$	$\text{CH}=\text{CH}_2/\text{C}(\text{CH}_3)=\text{CH}_2$	$\text{C}=\text{O}$	$\text{CH}_2\text{-O}$	S-CH_2
1	CHCl_3	131.23	128.02	165.77	62.75	31.86
	<i>CHCl_3</i>	147.15	128.61	172.28	68.79	39.49
	<i>$\text{DMSO-}d_6$</i>	147.79	128.92	173.92	69.25	39.60
2	CHCl_3	131.23	127.98	165.71	62.58	31.86
	<i>CHCl_3</i>	139.15	134.17	170.93	64.66	38.02
	<i>$\text{DMSO-}d_6$</i>	142.74	135.31	175.04	66.37	39.31
3	CHCl_3	131.25	127.90	165.57	62.46	31.75
	<i>CHCl_3</i>	139.45	133.77	173.98	65.01	37.26
	<i>$\text{DMSO-}d_6$</i>	142.79	135.30	175.07	66.44	39.34
4	CHCl_3	125.97	135.98	167.01	62.92	31.93
	<i>CHCl_3</i>	148.30	143.64	171.72	72.90	40.91
	<i>$\text{DMSO-}d_6$</i>	148.57	144.15	173.44	73.27	40.98
5	CHCl_3	126.05	122.18	167.01	62.73	31.98
	<i>CHCl_3</i>	138.00	147.64	177.07	67.76	37.13
	<i>$\text{DMSO-}d_6$</i>	137.10	146.94	175.34	66.24	35.53
6	CHCl_3	126.05	135.92	166.95	62.69	31.93
	<i>CHCl_3</i>	138.15	148.23	176.98	68.08	40.00
	<i>$\text{DMSO-}d_6$</i>	136.40	146.98	175.24	66.38	39.53

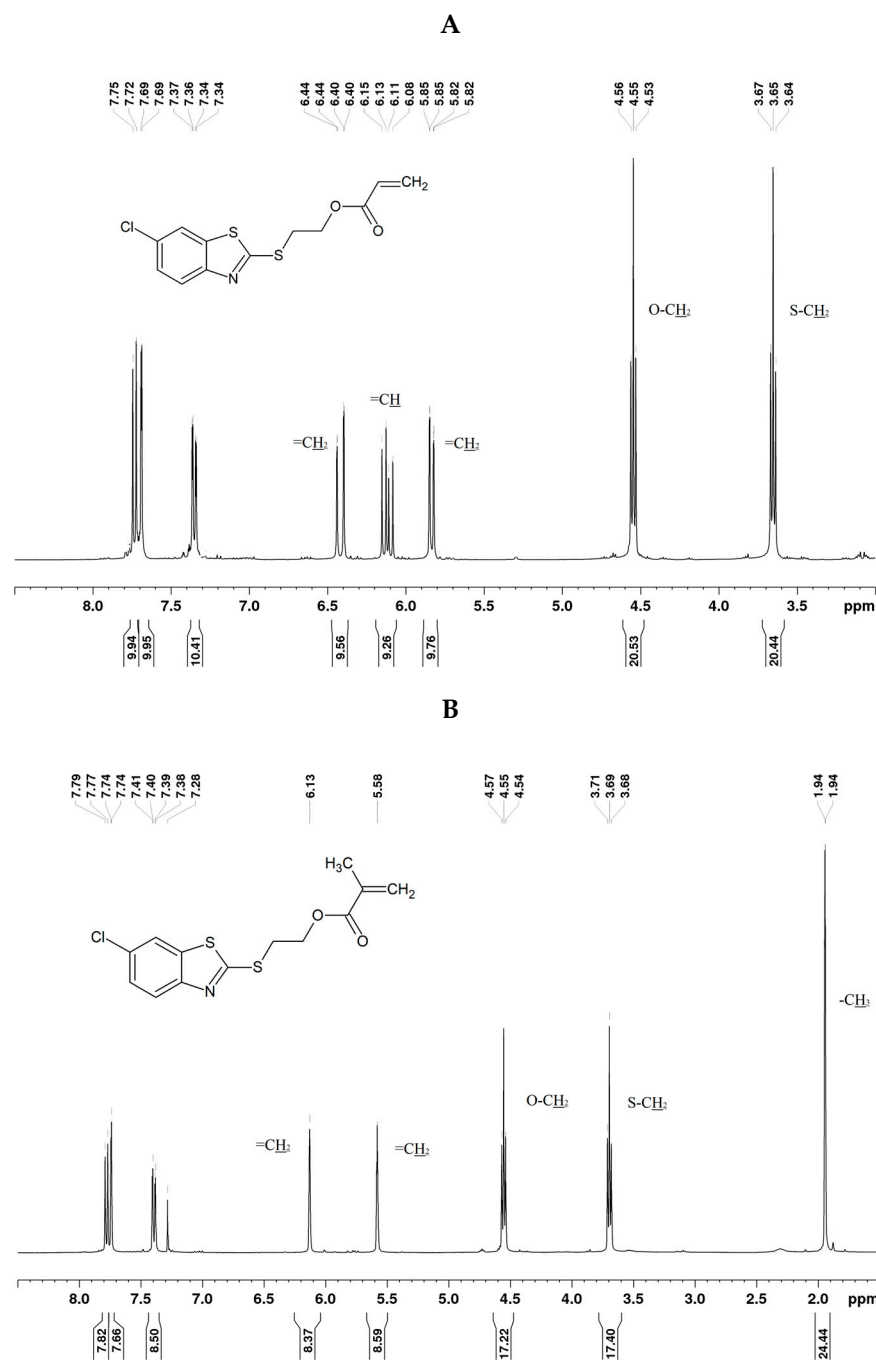


Figure 3. ^1H NMR spectrum (400 MHz) of 2-(2-(6-chlorobenzothiazolyl)thio)ethyl acrylate (2) (A) and 2-(2-(6-chlorobenzothiazolyl)thio)ethyl methacrylate (5) in CDCl_3 (B).

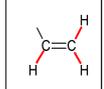
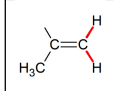
In the ^{13}C NMR spectra, the most downfield peak corresponds to the carbonyl carbon atom $\text{C}=\text{O}$, resonating at approximately 165 ppm for acrylic (1–3) and approximately 167 ppm for methacrylic 2-mercaptobenzothiazole derivatives (4–6). On the most shielded part of the spectrum, the chemical shifts of carbons in alkane groups were observed. The chemical shifts of $\text{CH}_2\text{-O}$ and $\text{CH}_2\text{-S}$ resonated at around 63 ppm and 32 ppm, respectively (Supplementary Materials). Consistent with the ^1H NMR spectra, these chemical shift values for all carbon atoms align with those previously described for related compounds [42].

Chemical shift values were computed to validate the experimental data. Both ^1H and ^{13}C NMR chemical shift values fell within the calculated range. The deviations observed were attributed to the common use of dimethyl sulfoxide instead of chloroform during calculations, demonstrating the impact of changing the solvent on chemical shift values.

3.2. Vibrational Analysis

In the identification of new chemical compounds, infrared (IR) spectroscopy serves as one of several tools. When combined with techniques such as nuclear magnetic resonance (NMR) spectroscopy, IR spectroscopy enhances the comprehensive understanding of the properties of a compound. For the study of the title compounds, vibrational spectroscopy and quantum chemical calculations using the B3LYP functional and 6–311+G(d,p) basis set were employed. Sharp bands of strong intensity, observed at 1714–1721 cm^{-1} (calculated values: 1769–1795 cm^{-1}), in the analyzed spectra of compounds were attributed to stretching vibrations of the C=O group. Additionally, in the range of 1632–1636 cm^{-1} (calculated values: 1653–1689 cm^{-1}), the characteristic band of (C=C) vibrations of alkene fragments was observed. The most characteristic vibrational bands are summarized in Table 3.

Table 3. Characteristic band strength values of the synthesized compounds.

Compounds	ν_s and ν_{as} (C–H)		ν_s and ν_{as} (C–H)		ν (C=O)	ν (C=C)
		or 				
1		3031–3425		2860–2951	1720	1632
2		3036–3435		2690–2946	1720	1633
3		3035–3435		2658–2947	1721	1634
4		2950–3021		2734–2922	1715	1636
5		2951–3021		2734–2922	1715	1636
6		3066–3085		2836–2978	1714	1636

3.3. Spectroscopic Studies

The compounds under study, akin to those previously examined [42], exhibited distinct absorption in the wavelength range from 260 to 350 nm. Solvent polarity showed a weak impact on the position of maximum absorption. However, a slight shift toward a lower wavelength was noticeable when methanol was used (Figure 4A). The transition from acrylic (compounds 1–3) to methacrylic (compounds 4–6) did not significantly affect the position of the absorption band (Figure 4B), which was primarily influenced by the type and position of the substituent attached to the phenyl group. In general, the shape of the absorption spectrum and the position of its maximum do not depend on the type of substituent, but on its place. The presence of chlorine at locant six on the benzene ring of 2-mercaptobenzothiazole (compound 2 and 5) resulted in slight shifts toward higher wavelengths (bathochromic shift) compared to the compound with the same substituent at position five (3 and 6) (Figure 4C). The molar absorption coefficient (ϵ) in the 1–6 series varied between 8800 and 16,200 $\text{M}^{-1}\cdot\text{cm}^{-1}$ (Table 4). The spectroscopic characteristics of the compounds studied are presented in Table 4.

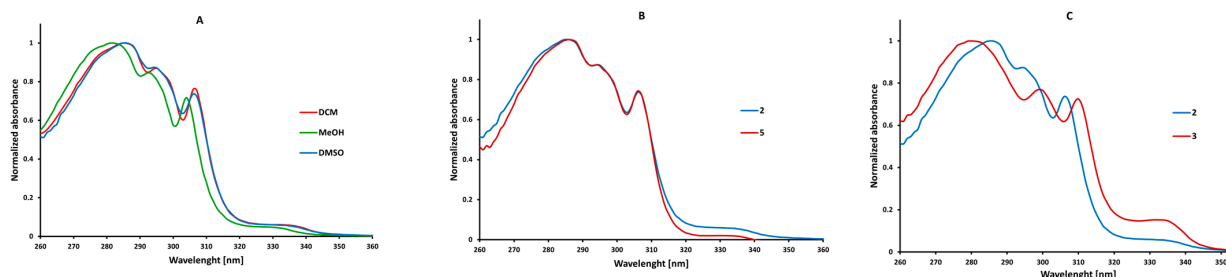


Figure 4. Normalized absorption spectra of: 2-(2-(6-chlorobenzothiazolyl)thio)ethyl acrylate (2) in solvents of different polarities (A), 2-(2-(6-chlorobenzothiazolyl)thio)ethyl acrylate (2) and 2-(2-(6-chlorobenzothiazolyl)thio)ethyl methacrylate (5) in dimethyl sulfoxide (B), and 2-(2-(6-chlorobenzothiazolyl)thio)ethyl acrylate (2) and 2-(2-(5-chlorobenzothiazolyl)thio)ethyl acrylate (3) in dimethyl sulfoxide (C).

Table 4. Measured and calculated spectroscopic data for 2-(2-benzothiazolylthio)ethyl acrylate derivatives (1–3) and methacrylate derivatives (4–6) in selected solvents of different polarities.

Compound	Solvent	λ_{ab} (nm) (Measured)	λ_{ab} (nm) (Calculated)	ϵ ($\times 10^4$, $M^{-1} \cdot cm^{-1}$)
1	DCM	283	278	1.21
	MeOH	282	278	1.14
	DMSO	285	279	1.21
2	DCM	285	282	1.21
	MeOH	283	281	1.32
	DMSO	285	282	1.15
3	DCM	279	283	1.16
	MeOH	278	282	0.88
	DMSO	280	283	1.45
4	DCM	285	279	1.42
	MeOH	282	278	1.30
	DMSO	285	279	1.17
5	DCM	285	282	1.62
	MeOH	283	281	1.48
	DMSO	286	282	1.56
6	DCM	279	281	1.32
	MeOH	277	281	1.10
	DMSO	279	282	1.23

3.4. Computational Details

The HOMO (Highest Occupied Molecular Orbital) and LUMO (Lowest Unoccupied Molecular Orbital) values provide insights into the energy levels of molecular orbitals within a given molecule. This information is crucial for comprehending the chemical properties of molecules, reactivity, and behavior in chemical reactions. Similar to the previously tested compounds [42], the calculations indicated that the derivatives with electron-donating groups exhibited the highest reactivity (compounds 1 and 4). Such molecules showed the lowest values of hardness and energy gaps (Table 5). Additionally, the higher energy gap values of 2-(2-benzothiazolylthio)ethyl methacrylate derivatives (4–6) suggest that they may be less reactive than their acrylic counterparts (1–3) (Figure 5). Notably, there was no evident impact of solvent polarity on the calculated parameters.

Table 5. The values of hardness (η), energy gap, and energies of HOMO and LUMO orbitals estimated for all compounds.

Compound	Solvent	HOMO (eV)	LUMO (eV)	Energy Gap (eV)	η (eV)
1	DCM	−6.1358	−1.9627	4.1731	2.0865
	MeOH	−6.1415	−1.9508	4.1908	2.0954
	DMSO	−6.1423	−1.9497	4.1927	2.0963
2	DCM	−6.2863	−1.8019	4.4844	2.2422
	MeOH	−6.2822	−1.7916	4.4906	2.2453
	DMSO	−6.2819	−1.7905	4.4914	2.2457
3	DCM	−6.3704	−1.8044	4.5660	2.2830
	MeOH	−6.3628	−1.7927	4.5701	2.2850
	DMSO	−6.3622	−1.7913	4.5709	2.2855
4	DCM	−6.1312	−1.8419	4.2893	2.1446
	MeOH	−6.1383	−1.8422	4.2961	2.1480
	DMSO	−6.1394	−1.8422	4.2972	2.1486
5	DCM	−6.2836	−1.6389	4.6446	2.3223
	MeOH	−6.2808	−1.6357	4.6452	2.3226
	DMSO	−6.2806	−1.6354	4.6452	2.3226
6	DCM	−6.3696	−1.6416	4.7279	2.3640
	MeOH	−6.3606	−1.6365	4.7241	2.3621
	DMSO	−6.3598	−1.6362	4.7236	2.3618

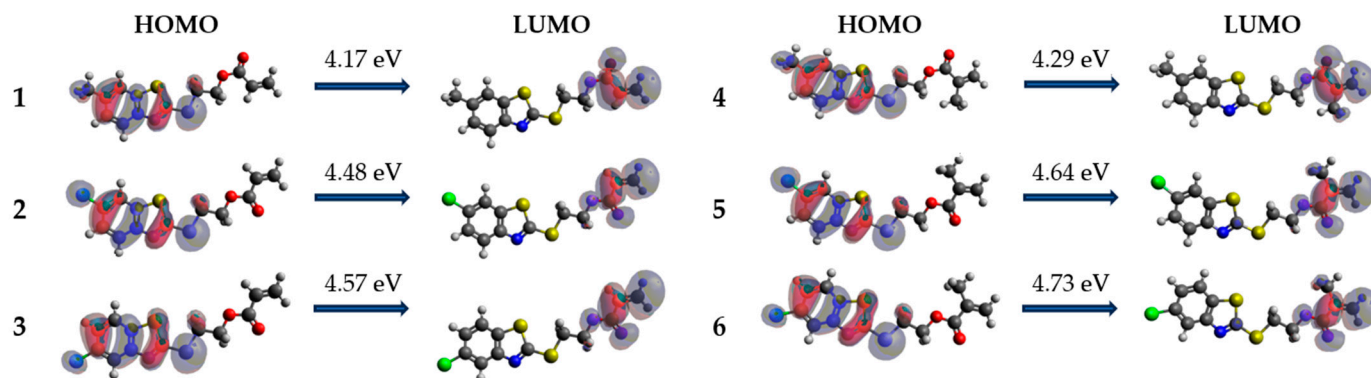


Figure 5. Frontier molecular diagram of 2-(2-benzothiazolylthio)ethyl acrylate (1–3) and methacrylate derivatives (4–6) in dichloromethane.

The activity of the photoinitiation of free-radical photopolymerization of the studied compounds will be confirmed by kinetic studies in a future paper.

4. Conclusions

The synthesis of novel 2-(2-benzothiazolylthio)ethyl acrylates (1–3) and methacrylates (4–6) is described here. The chemical structures of the synthesized compounds were confirmed by using various spectroscopic methods. Experimental spectroscopic data were effectively reproduced and complemented by quantum chemical DFT theoretical calculations. The study revealed that the replacement of the hydrogen atom in acrylate derivatives ($R^3 = H$ in Scheme 1) on the methyl group to methacrylate ($R^3 = CH_3$ in Scheme 1) had only a minor effect on their spectroscopic properties. In addition, it was shown that the solvent had a weak impact on the position of the absorption band, while the structure of the compound and the type and position of the substituent significantly influenced it. The substitution of the same substituent into the C6 (R^2 in Scheme 1) position of the phenyl ring of the 2-mercaptobenzothiazole resulted in a slight shift toward a higher wavelength (bathochromic shift) when compared to the compound with substitution into the C5 (R^1 in Scheme 1) position. The obtained HOMO and LUMO energy values indicated that 2-(2-benzothiazolylthio)ethyl acrylate derivatives (1–3) exhibited greater reactivity compared to 2-(2-benzothiazolylthio)ethyl methacrylate derivatives (4–6). Further investigations will be focused on studying the activity of new 2-mercaptobenzothiazole-based acrylates and methacrylates in photo-initiating systems for radical polymerization of acrylates.

Supplementary Materials: The following supporting information can be downloaded at: <https://www.mdpi.com/article/10.3390/ma17010246/s1>. Figure S1. 1H NMR spectrum (400 MHz) of 2-(2-(6-methylbenzothiazolyl)thio)ethyl acrylate (1) in $CDCl_3$; Figure S2. ^{13}C NMR spectrum (400 MHz) of 2-(2-(6-methylbenzothiazolyl)thio)ethyl acrylate (1) in $CDCl_3$; Figure S3. 1H NMR spectrum (400 MHz) of 2-(2-(6-chlorobenzothiazolyl)thio)ethyl acrylate (2) in $CDCl_3$; Figure S4. ^{13}C NMR spectrum (400 MHz) of 2-(2-(6-chlorobenzothiazolyl)thio)ethyl acrylate (2) in $CDCl_3$; Figure S5. 1H NMR spectrum (400 MHz) of 2-(2-(5-chlorobenzothiazolyl)thio)ethyl acrylate (3) in $CDCl_3$; Figure S6. ^{13}C NMR spectrum (400 MHz) of 2-(2-(5-chlorobenzothiazolyl)thio)ethyl acrylate (3) in $CDCl_3$; Figure S7. 1H NMR spectrum (400 MHz) of 2-(2-(6-methylbenzothiazolyl)thio)ethyl methacrylate (4) in $CDCl_3$; Figure S8. ^{13}C NMR spectrum (400 MHz) of 2-(2-(6-methylbenzothiazolyl)thio)ethyl methacrylate (4) in $CDCl_3$; Figure S9. 1H NMR spectrum (400 MHz) of 2-(2-(6-chlorobenzothiazolyl)thio)ethyl methacrylate (5) in $CDCl_3$; Figure S10. ^{13}C NMR spectrum (400 MHz) of 2-(2-(6-chlorobenzothiazolyl)thio)ethyl methacrylate (5) in $CDCl_3$; Figure S11. 1H NMR spectrum (400 MHz) of 2-(2-(5-chlorobenzothiazolyl)thio)ethyl methacrylate (6) in $CDCl_3$; Figure S12. ^{13}C NMR spectrum (400 MHz) of 2-(2-(5-chlorobenzothiazolyl)thio)ethyl methacrylate (6) in $CDCl_3$; Figure S13. Chromatogram of 2-(2-(6-methylbenzothiazolyl)thio)ethyl acrylate (1); Figure S14. Mass spectrum of 2-(2-(6-methylbenzothiazolyl)thio)ethyl acrylate (1); Figure S15. Chromatogram of 2-(2-(6-chlorobenzothiazolyl)thio)ethyl acrylate (2); Figure S16. Mass spectrum of 2-(2-(6-chlorobenzothiazolyl)thio)ethyl acrylate (2); Figure S17. Chromatogram of 2-(2-(5-

chlorobenzothiazolyl)thio)ethyl acrylate (3); Figure S18. Mass spectrum of 2-(2-(5-chlorobenzothiazolyl)thio)ethyl acrylate (3); Figure S19. Chromatogram of 2-(2-(6-methylbenzothiazolyl)thio)ethyl methacrylate (4); Figure S20. Mass spectrum of 2-(2-(6-methylbenzothiazolyl)thio)ethyl methacrylate (4); Figure S21. Chromatogram of 2-(2-(6-chlorobenzothiazolyl)thio)ethyl methacrylate (5); Figure S22. Mass spectrum of 2-(2-(6-chlorobenzothiazolyl)thio)ethyl methacrylate (5); Figure S23. Chromatogram of 2-(2-(5-chlorobenzothiazolyl)thio)ethyl methacrylate (6); Figure S24. Mass spectrum of 2-(2-(5-chlorobenzothiazolyl)thio)ethyl methacrylate (6).

Author Contributions: Conceptualization, J.K.-B. and A.S.; methodology, A.S.; software, A.S.; validation, A.S.; investigation, A.S.; ab initio calculations, A.S.; resources, A.S.; data curation, A.S.; writing—original draft preparation, A.S.; writing—review, J.K.-B. and A.S.; funding acquisition, J.K.-B. and A.S. All authors have read and agreed to the published version of the manuscript.

Funding: This research was funded in part by the National Science Centre, Poland, grant number 2022/06/X/ST4/00581. For the purpose of Open Access, the authors have applied a CC-BY public copyright license to any Author-Accepted Manuscript versions arising from this submission.

Institutional Review Board Statement: Not applicable.

Informed Consent Statement: Not applicable.

Data Availability Statement: The RepOD Open Data Repository (<https://doi.org/10.18150/R9VGVW9>) contains raw data and metadata related to the spectral characteristics of 2-mercaptobenzothiazole derivatives.

Acknowledgments: This research was supported by PL-Grid Infrastructure (<http://www.plgrid.pl/en> (accessed on 15 November 2023)).

Conflicts of Interest: The authors declare no conflict of interest.

References

1. Azam, M.A.; Suresh, B. Biological activities of 2-mercaptobenzothiazole derivatives: A review. *Sci. Pharm.* **2012**, *80*, 789–823. [[CrossRef](#)] [[PubMed](#)]
2. Shafi, S.; Mahboob Alam, M.; Mulakayala, N.; Mulakayala, C.; Vanaja, G.; Kalle, A.M.; Pallu, R.; Alam, M.S. Synthesis of novel 2-mercapto benzothiazole and 1,2,3-triazole based bis-heterocycles: Their anti-inflammatory and anti-nociceptive activities. *Eur. J. Med. Chem.* **2012**, *49*, 324–333. [[CrossRef](#)] [[PubMed](#)]
3. Gulab, H.; Shah, Z.; Mahmood, M.; Shah, S.R.; Ali, S.; Iqbal, M.; Khan, M.N.; Flörke, U.; Khan, S.A. Synthesis, characterization and antibacterial activity of a new calcium complex using sodium 2-mercaptobenzothiazole and 1,10-phenanthroline as ligands. *J. Mol. Struct.* **2018**, *1154*, 140–144. [[CrossRef](#)]
4. Fong, J.; Yuan, M.; Jakobsen, T.H.; Mortensen, K.T.; Delos Santos, M.M.S.; Chua, S.L.; Yang, L.; Tan, C.H.; Nielsen, T.E.; Givskov, M. Disulfide Bond-Containing Ajoene Analogues As Novel Quorum Sensing Inhibitors of *Pseudomonas aeruginosa*. *J. Med. Chem.* **2017**, *60*, 215–227. [[CrossRef](#)] [[PubMed](#)]
5. Cano, N.H.; Ballari, M.S.; López, A.G.; Santiago, A.N. New Synthesis and Biological Evaluation of Benzothiazole Derivates as Antifungal Agents. *J. Agric. Food Chem.* **2015**, *63*, 3681–3686. [[CrossRef](#)] [[PubMed](#)]
6. Yadav, K.P.; Rahman, M.A.; Nishad, S.; Maurya, S.K.; Anas, M.; Mujahid, M. Synthesis and biological activities of benzothiazole derivatives: A review. *Intell. Pharm.* **2023**, *1*, 122–132. [[CrossRef](#)]
7. Sun, X.; Liu, S.; Hu, P.; Sun, S.; Xie, Z.; Hu, G.; Hu, D.; Zhang, M. Microscale Corrosion Inhibition Behavior of Four Corrosion Inhibitors (BTA, MBI, MBT, and MBO) on Archeological Silver Artifacts Based on Scanning Electrochemical Cell Microscopy. *Anal. Chem.* **2023**, *95*, 14686–14694. [[CrossRef](#)]
8. Garg, V.; Sharma, S.B.; Zanna, S.; Seyeux, A.; Wiame, F.; Maurice, V.; Marcus, P. Enhanced corrosion inhibition of copper in acidic environment by cathodic control of interface formation with 2-mercaptobenzothiazole. *Electrochim. Acta* **2023**, *447*, 142162. [[CrossRef](#)]
9. Vernack, E.; Zanna, S.; Seyeux, A.; Costa, D.; Chiter, F.; Tingaut, P.; Marcus, P. ToF-SIMS, XPS and DFT study of the adsorption of 2-mercaptobenzothiazole on copper in neutral aqueous solution and corrosion protection in chloride solution. *Corros. Sci.* **2023**, *210*, 110854. [[CrossRef](#)]
10. Finšgar, M.; Čakara, D. Spectroscopic analysis and in situ adsorption of 2-mercaptobenzothiazole corrosion inhibitor on Zn from a chloride solution. *Appl. Surf. Sci.* **2022**, *606*, 154843. [[CrossRef](#)]
11. Eduok, U.; Faye, O.; Szpunar, J.; Khaled, M. CS₂ mediated synthesis of corrosion-inhibiting mercaptobenzothiazole molecule for industrial zinc: Experimental studies and molecular dynamic simulations. *J. Mol. Liq.* **2021**, *324*, 115129. [[CrossRef](#)]
12. Chiter, F.; Costa, D.; Maurice, V.; Marcus, P. Chemical interaction, self-ordering and corrosion inhibition properties of 2-mercaptobenzothiazole monolayers: DFT atomistic modeling on metallic copper. *Corros. Sci.* **2022**, *209*, 110658. [[CrossRef](#)]

13. Majidi, R.; Danaee, I.; Vrsalović, L.; Zarei, D. Development of a smart anticorrosion epoxy coating containing a pH-sensitive GO/MOF nanocarrier loaded with 2-mercaptobenzothiazole corrosion inhibitor. *Mater. Chem. Phys.* **2023**, *308*, 128291. [CrossRef]
14. He, S.; Gao, Y.; Wu, C.; Chen, Z.; Cen, H. A self-healing and anticorrosion epoxy coating based on the novel polymer filler containing a side-linked grafting 2-mercaptobenzothiazole. *J. Mater. Res. Technol.* **2023**, *26*, 1107–1121. [CrossRef]
15. Nawaz, M.; Kahraman, R.; Taryba, M.G.; Hassan, M.K.; Attaei, M.; Montemor, M.F.; Shakoor, R.A. Improved properties of polyolefin nanocomposite coatings modified with ceria nanoparticles loaded with 2-mercaptobenzothiazole. *Prog. Org. Coat.* **2022**, *171*, 107046. [CrossRef]
16. Larsson, L.F.G.; Tractz, G.T.; Camargo Matheus, A.P.; Pinto Rodrigues, P.R. The use of 2-Mercaptobenzothiazole as a new co-adsorbent in dye-sensitized solar cells. *Opt. Mater.* **2022**, *131*, 112658. [CrossRef]
17. Rojruthai, P.; Sakdapipanich, J.; Wiriyantawong, J.; Ho, C.C.; Chaiear, N. Effect of Latex Purification and Accelerator Types on Rubber Allergens Prevalent in Sulphur Pre-vulcanized Natural Rubber Latex: Potential Application for Allergy-Free Natural Rubber Gloves. *Polymers* **2022**, *14*, 4679. [CrossRef]
18. Zhao, J.; Cheng, X.; Wang, L.; Wang, J.; Song, C. Hydrogenation of tar residue derived from the synthesis of rubber vulcanization accelerator 2-mercaptobenzothiazole. *Asia-Pac. J. Chem. Eng.* **2017**, *12*, 400–405. [CrossRef]
19. Morgan, B.; McGill, W.J. 2-Mercaptobenzothiazole as Accelerator for 2,3-Dimethyl-2-butene. *J. Appl. Polym. Sci.* **2000**, *76*, 1377–1385. [CrossRef]
20. Van Der Horst, M.; Hendrikse, K.G.; Woolard, C.D. The role of thiol intermediates in 2-mercaptobenzothiazole accelerated sulfur vulcanization of rubber model compounds. *J. Appl. Polym. Sci.* **2003**, *89*, 47–54. [CrossRef]
21. Andrzejewska, E.; Zych-Tomkowiak, D.; Andrzejewski, M.; Hug, G.L.; Marciniak, B. Heteroaromatic thiols as co-initiators for type II photoinitiating systems based on camphorquinone and isopropylthioxanthone. *Macromolecules* **2006**, *39*, 3777–3785. [CrossRef]
22. Degirmenci, A.; Sanyal, R.; Arslan, M.; Sanyal, A. Benzothiazole-disulfide based redox-responsive polymers: Facile access to reversibly functionalizable polymeric coatings. *Polym. Chem.* **2022**, *13*, 2595–2607. [CrossRef]
23. Pirman, T.; Ocepek, M.; Likozar, B. Radical Polymerization of Acrylates, Methacrylates, and Styrene: Biobased Approaches, Mechanism, Kinetics, Secondary Reactions, and Modeling. *Ind. Eng. Chem. Res.* **2021**, *60*, 9347–9367. [CrossRef]
24. Chen, Y.; Jia, Q.; Ding, Y.; Sato, S.I.; Xu, L.; Zang, C.; Shen, X.; Kakuchi, T. B(C6F5)3-Catalyzed Group Transfer Polymerization of Acrylates Using Hydrosilane: Polymerization Mechanism, Applicable Monomers, and Synthesis of Well-Defined Acrylate Polymers. *Macromolecules* **2019**, *52*, 844–856. [CrossRef]
25. Brydson, J.A. *Plastic Materials*, 7th ed.; Butterworth-Heinemann: Oxford, UK, 1999; ISBN 9780750641326.
26. Su, H.W.; Chen, W.C.; Lee, W.C.; King, J.S. New photocurable acrylic/silsesquioxane hybrid optical materials: Synthesis, properties, and patterning. *Macromol. Mater. Eng.* **2007**, *292*, 666–673. [CrossRef]
27. Montheard, J.-P.; Chatzopoulos, M.; Chappard, D. 2-Hydroxyethyl Methacrylate (HEMA): Chemical Properties and Applications in Biomedical Fields. *J. Macromol. Sci. Part C* **1992**, *32*, 1–34. [CrossRef]
28. Feng, M.; Sefton, M. V Hydroxyethyl methacrylate–methyl methacrylate (HEMA–MMA) copolymers for cell microencapsulation: Effect of HEMA purity. *J. Biomater. Sci. Polym. Ed.* **2000**, *11*, 537–545. [CrossRef]
29. Huang, J.; Lean, J. Advances in acrylic structural adhesives. In *Advances in Structural Adhesive Bonding*, 2nd ed.; Woodhead Publishing: Sawston, UK, 2023; pp. 69–101, ISBN 9780323912143.
30. Mori, H.; Müller, A.H.E. New polymeric architectures with (meth)acrylic acid segments. *Prog. Polym. Sci.* **2003**, *28*, 1403–1439. [CrossRef]
31. Corsaro, C.; Neri, G.; Santoro, A.; Fazio, E. Acrylate and Methacrylate Polymers' Applications: Second Life with Inexpensive and Sustainable Recycling Approaches. *Materials* **2022**, *15*, 282. [CrossRef]
32. Parra, F.; Vázquez, B.; Benito, L.; Barcenilla, J.; San Román, J. Foldable antibacterial acrylic intraocular lenses of high refractive index. *Biomacromolecules* **2009**, *10*, 3055–3061. [CrossRef]
33. Cracium, L.; Polishchuk, O.; Schriver, G.W.; Hainz, R. High Refractive Index Monomers, Compositions and Uses Thereof. U.S. Patent 2008/0200582 A1, 21 August 2008.
34. Chisholm, B.J.; Pickett, J.E. Method of Making a High Refractive Index Optical Management Coating and the Coating. U.S. Patent 7,045,558 B2, 15 May 2006.
35. Ong, B.K.; Woon, K.L.; Ariffin, A. Evaluation of various density functionals for predicting the electrophosphorescent host HOMO, LUMO and triplet energies. *Synth. Met.* **2014**, *195*, 54–60. [CrossRef]
36. Becke, A.D. Density-functional thermochemistry. III. The role of exact exchange. *J. Chem. Phys.* **1993**, *98*, 5648. [CrossRef]
37. Lee, C.; Yang, W.; Parr, R.G. Development of the Colle-Salvetti correlation-energy formula into a functional of the electron density. *Phys. Rev. B* **1988**, *37*, 785–789. [CrossRef] [PubMed]
38. Petersson, G.A.; Al-Laham, M.A. A complete basis set model chemistry. II. Open-shell systems and the total energies of the first-row atoms. *J. Chem. Phys.* **1991**, *94*, 6081–6090. [CrossRef]
39. Petersson, G.A.; Bennett, A.; Tensfeldt, T.G.; Al-Laham, M.A.; Shirley, W.A.; Mantzaris, J. A complete basis set model chemistry. I. The total energies of closed-shell atoms and hydrides of the first-row elements. *J. Chem. Phys.* **1988**, *89*, 2193–2218. [CrossRef]
40. Frisch, M.J.; Trucks, G.W.; Schlegel, H.B.; Scuseria, G.E.; Robb, M.A.; Cheeseman, J.R.; Scalmani, G.; Barone, V.; Petersson, G.A.; Nakatsuji, H.; et al. Gaussian, Inc., Wallingford, CT, USA. 2016. Available online: <https://gaussian.com/g09citation/> (accessed on 25 December 2023).

41. Hanwell, M.D.; Curtis, D.E.; Lonie, D.C.; Vandermeersch, T.; Zurek, E.; Hutchison, G.R. Avogadro: An advanced semantic chemical editor, visualization, and analysis platform. *J. Cheminform.* **2012**, *4*, 17. [[CrossRef](#)]
42. Kabatc-Borcz, J.; Czeleń, P.; Skotnicka, A. Synthesis and Spectroscopic Properties of Selected Acrylic and Methacrylic Derivatives of 2-Mercaptobenzothiazole. *Symmetry* **2023**, *15*, 370. [[CrossRef](#)]

Disclaimer/Publisher's Note: The statements, opinions and data contained in all publications are solely those of the individual author(s) and contributor(s) and not of MDPI and/or the editor(s). MDPI and/or the editor(s) disclaim responsibility for any injury to people or property resulting from any ideas, methods, instructions or products referred to in the content.